IJST, Transactions of Civil Engineering, Vol. 38, No. C1+, pp 157-173
Printed in The Islamic Republic of Iran, 2014

AN ANISOTROPIC DAMAGE MODEL FOR METALS BASED ON IRREVERSIBLE THERMODYNAMICS FRAMEWORK*

H. AZIZSOLTANI[1**], M. T. KAZEMI[2] AND M. R. JAVANMARDI[3]

[1, 2]Dept. of Civil Engineering, Sharif University of Technology, Tehran, I. R. of Iran
Email: hasoltani@alum.sharif.edu
[3]Dept. of Civil Engineering, Shiraz University, Shiraz, I. R. of Iran

Abstract– In this article, a model of anisotropic damage coupled to plasticity based on thermodynamics framework is proposed. This model is introduced to describe the plastic and damage behavior of metals adequately. According to the elastic energy equivalence hypothesis between the undamaged material and the damaged material, the constitutive equations for the material in damaged configuration are written. The damaged material is modeled using the constitutive laws of the undamaged material in which the stresses in undamaged configuration are mapped by the stresses in damaged configuration. The damage is proposed through a damage mechanics framework, and the material degradation is determined by utilizing an anisotropic damage measure. In developing constitutive model, a plastic yield surface is used to demonstrate the onset of plasticity, and a damage surface is used to demonstrate the onset of damage.

The plastic relationships have been written in undamaged configuration, and by using relationships between damaged and undamaged configurations, plastic equations are extended to damaged configuration.

Numerical simulations of the elastoplastic deformation behavior of hydrostatic stress sensitive metals demonstrate the efficiency of the formulation, and also show the physical effects of parameters of the model. In order to achieve an equilibrated global solution, a nonlinear finite element program that employs a Newton Raphson iteration procedure is applied. Finally, the numerical results of some examples are validated with the existing experimental measurements.

Keywords– Anisotropic damage, thermodynamics framework, damage configuration

1. INTRODUCTION

Inelastic deformations in polycrystalline metals are accompanied by internal damage that is dependent on the growth of microdefects - microvoids, microcracks - in material [1-2]. Theses damage processes begin in some states of deformation, and its evolution depends mainly on the state of stress and strain.

Growth of microdefects will influence the elastic and plastic properties of the material; and this change of material characteristics such as elasticity modulus was not considered in classical plasticity theory. However, by using damage models, this modification can be considered. Anisotropic damage models require using continuous mechanics besides thermodynamics framework and kinematic variables. Combinations of plasticity and damage are usually based on isotropic hardening combined with one of the damage variables - isotropic, vectorial, or anisotropic damage. Based on effective strain in damaged materials, Kachanov [3] proposed primary concept of continuum damage mechanics; thus, researchers have chosen isotropic damage due to its simplicity and efficiency [3-5], axial vector representation of damage variables [6], and second order damage tensor [7-9].

*Received by the editors February 20, 2012; Accepted October 19, 2013
**Corresponding author

Damage and plastic deformation in materials have interaction with each other, which should be considered in modeling. In this paper, two surfaces including damage and plastic surfaces with a non-associated flow rule for plastic surface and an associated flow rule for damage surface are adopted.

2. ANISOTROPIC DAMAGE MODEL

Anisotropic damage can be used to model specific void and crack surfaces, specific crack and void volumes, or the spacing between cracks or voids. Increase in stress and deformation in metals leads to growth in microdefects that influences the elastic and plastic properties of the material. In this research, the plasticity theory has been applied to create consistency equations in undamaged configuration. These equations are extended to damage configuration by using relationships between undamaged and damaged configurations that Cordebois and Sidoroff [10] originally proposed.

In this model, two different types of configurations are utilized, including undamaged configurations and damaged ones. The former one is designated by superimposed dash, and the latter is designated without superimposed dash. Generally, the relationship between undamaged and damaged configuration in material is presented as follows [10-11]:

$$\bar{\sigma}_{ij} = M_{ijkl}\sigma_{kl} \tag{1}$$

where σ_{kl} is stress tensor in damaged configuration, $\bar{\sigma}_{ij}$ is stress tensor in undamaged configuration, and M_{ijkl} is fourth order damage effect tensor. In the present work, it is preferable to utilize fourth order damage effect tensor presented by Cordebois and Sidoroff [10]:

$$M_{ijkl} = \frac{1}{2}\left(\delta_{il}w_{kj} + w_{il}\delta_{kj}\right) \tag{2}$$

$$w_{ij} = (\delta_{ij} - \varphi_{ij})^{-1} \tag{3}$$

where δ_{ij} is the Kronecker delta, and φ_{ij} is second order damage tensor. For a general case of anisotropic damage, the second order damage tensor can be written in terms of damage densities [12]:

$$\varphi = \begin{bmatrix} \varphi_{11} & \varphi_{12} & \varphi_{13} \\ \varphi_{21} & \varphi_{22} & \varphi_{23} \\ \varphi_{31} & \varphi_{32} & \varphi_{33} \end{bmatrix} = \begin{bmatrix} d_1 & \sqrt{d_1 d_2} & \sqrt{d_1 d_3} \\ \sqrt{d_2 d_1} & d_2 & \sqrt{d_2 d_3} \\ \sqrt{d_3 d_1} & \sqrt{d_3 d_2} & d_3 \end{bmatrix} \tag{4}$$

Where d_i is microcracks density in i direction, and is described by the ratio of microcracks total area to surface total area whose unit normal is n_i.

The concept of elastic strain energy equivalence in undamaged and damaged configurations, firstly proposed by Chow and Wang [13], was applied to get stiffness tensor in damaged configurations:

$$\frac{1}{2}\sigma_{ij}\varepsilon^e_{ij} = \frac{1}{2}\bar{\sigma}_{ij}\bar{\varepsilon}^e_{ij} \tag{5}$$

With respect to generalized Hooke's law, the relation between stress and strain of isotropic material in elastic part for both configurations is expressed as follows:

$$\bar{\sigma}_{ij} = \bar{E}_{ijkl}\bar{\varepsilon}^e_{kl} \tag{6}$$

$$\sigma_{ij} = E_{ijkl}\varepsilon^e_{kl} \tag{7}$$

By substituting Eqs. (6) and (7) into Eq. (5), stiffness tensor in damaged configuration is obtained:

$$E_{ijkl} = M^{-1}_{ijmn}\bar{E}_{mnpq}M^{-T}_{pqkl} \tag{8}$$

By substituting Eqs. (6) and (7) into Eq. (1) and replacing E_{ijkl} from Eq. (8), the expression between elastic strain tensors in undamaged and damaged configurations can be obtained as follows:

$$\bar{\varepsilon}_{ij}^{e} = M_{ijkl}^{-T}\varepsilon_{kl}^{e} \tag{9}$$

where elastic strain tensor in damaged configurations (ε_{ij}^{e}) is the reversible part of strain in damaged configuration.

3. FRAMEWORK OF IRREVERSIBLE PROCESS

For the formulation of the constitutive and evolution equations of elastic, plastic and damage in materials, irreversible thermodynamics theory has been employed as a rational framework [14, 6].

In this research, thermodynamics operator based on the free potential proposed by Helmholtz is applied. These operators are presented in constant temperature. Clausius–Duhem inequality in isothermal condition can be written as follows [14]:

$$\sigma_{ij}\dot{\varepsilon}_{ij} - \rho\dot{\psi} \geq 0 \tag{10}$$

This inequality implies internal entropy production in an irreversible process, where ψ is Helmholtz free energy function that can be explained in terms of suitable internal state variables. In this work ψ is assumed to be a function of elastic strain tensor, equivalent plastic strain, second order damage tensor, and equivalent damage variable:

$$\psi = \psi\left(\varepsilon_{ij}^{e}, \bar{\varepsilon}^{ep}, \varphi_{ij}, \varphi^{eq}\right) \tag{11}$$

In this equation, elastic strain tensor (ε_{ij}^{e}) characterizes the behavior of elastic strain that represents reversible part of deformations. Equivalent plastic strain ($\bar{\varepsilon}^{ep}$) characterizes the plasticity isotropic hardening accumulated strain that represents irreversible part of deformations without taking into account generation and propagation of microdefects. Second order damage tensor (φ_{ij}) characterizes anisotropic damage in material that represents generation and propagation of microdefects. Equivalent (accumulated) damage variable (φ^{eq}) characterizes accumulated isotropic damage hardening that represents accumulated microdefects in material.

By taking time derivative of Eq. (11), substituting it into Eq. (10), and separating its reversible and irreversible parts, its reversible part can be obtained as follows:

$$\sigma_{ij} = \rho\frac{\partial\psi}{\partial\varepsilon_{ij}^{e}} \tag{12}$$

where ρ implies mass density; also, irreversible part leads to representing thermodynamic conjugate forces (Y_{ij}, K ,$\bar{C}$) that are respectively dependent on internal state variables (φ_{ij}, φ^{eq}, $\bar{\varepsilon}^{ep}$) [15]:

$$Y_{ij} = -\rho\frac{\partial\psi}{\partial\varphi_{ij}}, \qquad K = \rho\frac{\partial\psi}{\partial\varphi^{eq}}, \qquad \bar{C} = \rho\frac{\partial\psi}{\partial\bar{\varepsilon}^{ep}} \tag{13), (14), (15}$$

By defining mechanical flux vector (J), vector of conjugate forces (X) is expressed as follows:

$$J = \rho\left\{\dot{\varepsilon}_{ij}^{p}, \dot{\varphi}_{ij}, -\dot{\bar{\varepsilon}}^{ep}, -\dot{\varphi}^{eq}\right\}^{T} \tag{16}$$

$$X = \left\{\sigma_{ij}, Y_{ij}, \bar{C}, k\right\} \tag{17}$$

Rate of entropy production can be expressed as the scalar product of X and J as follows:

$$\sigma_{ij}\dot{\varepsilon}_{ij} - \rho\dot{\psi} = X.J \geq 0 \tag{18}$$

However, if a component of J (J_k) is assumed to be only a function of the corresponding thermodynamic force of X (X_k), the existence of dissipation potential functions can be proved [16].

$$F^p = F^p\left(\sigma_{ij}, \bar{C}, \dot{\varepsilon}^p_{ij}, \dot{\bar{\varepsilon}}^{ep}\right) \tag{19}$$

$$g = g\left(Y_{ij}, K, \dot{\varphi}_{ij}, \dot{\varphi}^{eq}\right) \tag{20}$$

where $F^p$and g are plastic and damage potential function, thus, J_k can be expressed as follows [16]:

$$\dot{\varepsilon}^p_{ij} = \dot{\lambda}^p \frac{\partial F^p}{\partial \sigma_{ij}}, \dot{\varphi}_{ij} = \dot{\lambda}^d \frac{\partial g}{\partial Y_{ij}}, \dot{\bar{\varepsilon}}^{ep} = \dot{\bar{\lambda}}^p \frac{\partial F^p}{\partial \bar{C}}, \dot{\varphi}^{eq} = \dot{\lambda}^d \frac{\partial g}{\partial K} \qquad (21), (22), (23), (24)$$

where $\dot{\lambda}^p$ and $\dot{\lambda}^d$are the plastic and damage loading factors that are known as the Lagrangian plasticity and damage multipliers, and can be obtained by plastic and damage consistency condition.

4. HELMHOLTZ FREE ENERGY FUNCTION

Helmholtz free energy function (ψ) is a portion of internal energy that is available for doing work at constant temperature. This function can be expressed as follows [14]:

$$\psi = u - s\theta \tag{25}$$

where u determines the specific internal energy, s is entropy and θ is the temperature. As it was mentioned in previous sections, increase in stress and deformation in material leads to growth of damage that influences the elastic and plastic properties of the material. Therefore, elastic strain energy of material is dependent on elastic strain and material damage [2].

In this research, Helmholtz free energy function has been assumed in three parts, including elastic, plastic, and damage. As it has been mentioned, elastic part is a function of elastic strain tensor (ε^e_{ij}) and second order damage tensor (φ_{ij}). Plastic and damage parts have been respectively assumed as functions of equivalent plastic strain ($\bar{\varepsilon}^{ep}$) and equivalent damage variable (φ^{eq}) [12, 17]:

$$\rho\psi\left(\varepsilon^e_{ij}, \bar{\varepsilon}^{ep}, \varphi_{ij}, \varphi^{eq}\right) = \rho\psi^e\left(\varepsilon^e_{ij}, \varphi_{ij}\right) + \rho\psi^p(\bar{\varepsilon}^{ep}) + \rho\psi^d(\varphi^{eq}) \tag{26}$$

a) Elastic part of Helmholtz free energy function:

To express elastic part of Helmholtz free energy function, elastic energy equality law proposed by Cordebois and Sidoroff [10] and expanded by Voyiadjis et al. [12] is used.

$$\rho\psi^e\left(\varepsilon^e_{ij}, \varphi_{ij}\right) = \frac{1}{2}\sigma_{ij}E^{-1}_{ijkl}\sigma_{kl} \tag{27}$$

By using Eqs. (13) and (8), thermodynamic conjugate force of second order damage tensor (φ_{ij}), that is Y_{ij}, is expressed as follows:

$$Y_{rs} = -\rho\frac{\partial\psi}{\partial\varphi_{rs}} = -\frac{1}{2}\sigma_{ij}\frac{\partial E^{-1}_{ijkl}}{\partial\varphi_{rs}}\sigma_{kl} \tag{28}$$

Solving Eq. (28) leads to the definition of Y_{rs}:

$$Y_{rs} = -\frac{1}{2}\sigma_{ij}\left(\frac{\partial M^T_{ijmn}}{\partial\varphi_{rs}}\bar{E}^{-1}_{mnpq}M_{pqkl} + M^T_{ijmn}\bar{E}^{-1}_{mnpq}\frac{\partial M_{pqkl}}{\partial\varphi_{rs}}\right)\sigma_{kl} \tag{29}$$

Moreover, with respect to M_{ijkl} which is a symmetric tensor, Y_{rs}can be written as:

$$Y_{rs} = -\sigma_{ij}\frac{\partial M_{ijmn}}{\partial \varphi_{rs}}\bar{E}^{-1}_{mnpq}M_{pqkl}\sigma_{kl} \tag{30}$$

b) Plastic part of Helmholtz free energy function:

The plastic part of Helmholtz free energy function expresses increase of free energy that is dependent on isotropic hardening in plastic deformation. For polycrystalline metals, plastic part of Helmholtz free energy function can be written as [18]:

$$\rho\psi^{p}(\bar{\varepsilon}^{ep}) = Q\left(\bar{\varepsilon}^{ep} + \frac{1}{Bc}e^{-Bc\bar{\varepsilon}^{ep}}\right) \tag{31}$$

where Q and Bc are material constants.

Substituting Eq. (15) into Eq. (31), thermodynamic conjugate force of $\bar{\varepsilon}^{ep}$, which is $\bar{C}$, can be obtained as follows:

$$\bar{C} = \rho\frac{\partial\psi}{\partial\bar{\varepsilon}^{ep}} = Q\left(1 - e^{-Bc\bar{\varepsilon}^{ep}}\right) \tag{32}$$

c) Damaged part of Helmholtz free energy function

The damaged part of Helmholtz free energy function is assumed to be a linear relationship between equivalent damage variable (φ^{eq}) and its thermodynamic conjugate force (K):

$$\rho\psi^{d}(\varphi^{eq}) = \frac{1}{2}K_{d}(\varphi^{eq})^{2} \tag{33}$$

By substituting Eq. (14) into Eq. (33), thermodynamic conjugate force of equivalent damage variable (φ^{eq}), which is *K*, can be obtained as follows:

$$K = \rho\frac{\partial\psi}{\partial\varphi^{eq}} = K_{d}\varphi^{eq} \tag{34}$$

5. ELASTOPLASTIC MODEL

Plasticity theory is used to express the behavior of various solids. In plasticity theory, a yield criterion is an assumption about determining the onset of the plastic deformation in material, and consistency condition imposes a restriction on the relationship between the stress and plastic strain tensor.

a) Plastic yield surface:

Spitzig et al. [19] carried out experimental studies on the effect of superimposed hydrostatic stress on the deformation behavior of metals, and Spitzig and Richmond [20] have shown that the flow stress depends approximately linearly on hydrostatic stress state. In this work, the model of Spitzig et al. [19] is extended to anisotropic damage by using two loading surfaces: one for plasticity and another for damage. Hence, the plastic yield condition of the iron base materials is as follows:

$$f\left(\bar{\sigma}_{ij}, \bar{\varepsilon}^{ep}\right) = \sqrt{\bar{J}_{2}} - (1 - \alpha\bar{I}_{1})\bar{C}_{(\bar{\varepsilon}^{ep})} = 0 \tag{35}$$

where $\bar{J}_{2} = \bar{s}_{ij}\bar{s}_{ij}/2$ is second invariant of the deviatoric stress tensor. $\bar{s}_{ij} = \bar{\sigma}_{ij} - \bar{\sigma}_{kk}\delta_{ij}/3$ is deviatoric stress tensor. $\bar{I}_{1} = \bar{\sigma}_{ii}$ is first invariant of the stress tensor. $\bar{\varepsilon}^{ep} = \int_{0}^{t}\dot{\bar{\varepsilon}}^{ep}dt$ is equivalent (accumulated) plastic strain. α is material constant, and $\bar{C}$ is expressed by Eq. (32) in terms of $\bar{\varepsilon}^{ep}$.

b) Non-associated flow rule

Incremental plastic strain vector in the strain space is normal to plastic potential function (F^p).

$$\dot{\bar{\varepsilon}}_{ij}^{p} = \dot{\bar{\lambda}}^{p} \frac{\partial F^{p}}{\partial \bar{\sigma}_{ij}} \tag{36}$$

Thus, the plastic potential function (F^p) is also formulated in terms of the stress tensor in undamaged configuration. In damaged metals, irreversible volumetric strains are mainly caused by damage, and volumetric plastic strains are negligible in comparison [19]. Thus, the plastic potential function is expressed as follows:

$$F^{p} = \sqrt{\bar{J}_2} \tag{37}$$

Then, the corresponding plastic flow direction ($\partial F^p / \partial \bar{\sigma}_{ij}$) is obtained as:

$$\frac{\partial F^{p}}{\partial \bar{\sigma}_{ij}} = \frac{\bar{S}_{ij}}{2\sqrt{\bar{J}_2}} \tag{38}$$

c) Incremental relationships between stress and strain in undamaged configuration

Since in plastic condition state of stress in material should be on the yield surface ($\dot{f} = 0$), the Kuhn Tucker plasticity consistency condition is expressed as follows [17]:

$$f \le 0\,, \quad \dot{\bar{\lambda}}^{p} \ge 0\,, \quad \dot{\bar{\lambda}}^{p} f = 0\,, \quad \dot{\bar{\lambda}}^{p} \dot{f} = 0 \tag{39}$$

By taking time derivative of Eq. (35), consistency condition can be expressed as follows:

$$\dot{f} = \frac{\partial f}{\partial \bar{\sigma}_{ij}} \dot{\bar{\sigma}}_{ij} + \frac{\partial f}{\partial \bar{\varepsilon}^{ep}} \dot{\bar{\varepsilon}}^{ep} = 0 \tag{40}$$

Differentiating the yield function with respect to σ_{ij} and again with respect to $\dot{\bar{\varepsilon}}^{ep}$gives:

$$\frac{\partial f}{\partial \bar{\sigma}_{ij}} = \frac{\bar{S}_{ij} \dfrac{(1-\alpha \bar{I}_1)}{2\sqrt{\bar{J}_2}} + \alpha \delta_{ij} \sqrt{\bar{J}_2}}{(1-\alpha \bar{I}_1)^2} \tag{41}$$

$$\frac{\partial f}{\partial \bar{\varepsilon}^{ep}} = \frac{\partial f}{\partial \bar{C}} \frac{\partial \bar{C}}{\partial \bar{\varepsilon}^{ep}} = -Bc(Q - \bar{C}) \tag{42}$$

By rearranging Eq. (35) in general form, that is,

$$f\left(\bar{\sigma}_{ij}, \bar{C}\right) = F\left(\bar{\sigma}_{ij}\right) - \bar{C}_{(\bar{\varepsilon}^{ep})} = 0 \tag{43}$$

$F\left(\bar{\sigma}_{ij}\right)$ is defined as:

$$F\left(\bar{\sigma}_{ij}\right) = \frac{\sqrt{\bar{J}_2}}{(1-\alpha \bar{I}_1)} \tag{44}$$

Defining effective stress in undamaged configuration as equal to stress that material yields in uniaxial loading and substituting effective stress in undamaged configuration ($\bar{\sigma}^e$) into Eq. (44), and solving it with respect to $\bar{\sigma}^e$, leads us to:

$$\bar{\sigma}^e = \frac{\sqrt{3\bar{J}_2}}{1-\alpha\bar{I}_1+\alpha\sqrt{3\bar{J}_2}} \tag{45}$$

Equating effective plastic work per unit volume to plastic work per unit volume, regarding both in undamaged configuration leads us to [17]:

$$dw_p = \overline{\sigma}^e \dot{\bar{\varepsilon}}^{ep} = \bar{\sigma}_{ij}\dot{\bar{\varepsilon}}^p_{ij} \tag{46}$$

Substituting Eqs. (36) and (45) into Eq. (46) leads us to the definition of the rate of the equivalent plastic strain:

$$\dot{\bar{\varepsilon}}^{ep} = \frac{1-\alpha\bar{I}_1+\alpha\sqrt{3\bar{J}_2}}{\sqrt{3\bar{J}_2}}\dot{\bar{\lambda}}^p\,\overline{\sigma}_{ij}\frac{\partial F^p}{\partial\overline{\sigma}_{ij}} \tag{47}$$

Time derivative of Eq. (6) besides decomposing strain tensor into elastic and plastic parts results in:

$$\dot{\bar{\sigma}}_{ij} = \bar{E}_{ijkl}\dot{\bar{\varepsilon}}^e_{kl} = \bar{E}_{ijkl}\left(\dot{\bar{\varepsilon}}_{kl} - \dot{\bar{\varepsilon}}^p_{kl}\right) \tag{48}$$

Substituting Eqs. (41), (42), (47), and (48) into Eq. (40) gives us plasticity consistency condition:

$$\dot{f} = \frac{\partial f}{\partial\bar{\sigma}_{ij}}\bar{E}_{ijkl}\dot{\bar{\varepsilon}}_{kl} - \dot{\bar{\lambda}}^p\frac{\partial f}{\partial\bar{\sigma}_{ij}}\bar{E}_{ijkl}\frac{\partial F^p}{\partial\overline{\sigma}_{kl}} + \dot{\bar{\lambda}}^p\frac{\partial f}{\partial\bar{C}}\frac{\partial\bar{C}}{\partial\bar{\varepsilon}^{ep}}\frac{1-\alpha\bar{I}_1+\alpha\sqrt{3\bar{J}_2}}{\sqrt{3\bar{J}_2}}\overline{\sigma}_{ij}\frac{\partial F^p}{\partial\overline{\sigma}_{ij}} = 0 \tag{49}$$

With regard to this equation, plastic multiplier in undamaged configuration ($\dot{\bar{\lambda}}^p$) is expressed as follows:

$$\dot{\bar{\lambda}}^p = \frac{1}{\bar{h}}\frac{\partial f}{\partial\bar{\sigma}_{ij}}\bar{E}_{ijkl}\dot{\bar{\varepsilon}}_{kl} \tag{50}$$

$$\overline{h} = \frac{\partial f}{\partial\bar{\sigma}_{ij}}\bar{E}_{ijkl}\frac{\partial F^p}{\partial\overline{\sigma}_{kl}} + \frac{\partial f}{\partial\bar{C}}\frac{\partial\bar{C}}{\partial\bar{\varepsilon}^{ep}}\frac{1-\alpha\bar{I}_1+\alpha\sqrt{3\bar{J}_2}}{\sqrt{3\bar{J}_2}}\overline{\sigma}_{ij}\frac{\partial F^p}{\partial\overline{\sigma}_{ij}} \tag{51}$$

By substituting Eqs. (36) and (50) into Eq. (48), elastoplastic tangent operator is defined as follows:

$$\overline{D}_{ijkl} = \bar{E}_{ijkl} - \frac{1}{\bar{h}}\bar{E}_{ijrs}\frac{\partial F^p}{\partial\bar{\sigma}_{rs}}\frac{\partial f}{\partial\bar{\sigma}_{mn}}\bar{E}_{mnkl} \tag{52}$$

6. ELASTOPLASTIC MODEL IN DAMAGED CONFIGURATION

In the previous section, elastoplastic model in undamaged configuration was presented. In this section, by using relationships between undamaged and damaged configurations, elastoplastic model in undamaged configuration is mapped to damaged configuration.

a) Damage surface

In this article, to obtain damage relationships, damage surface that was proposed by Chow and Wang [13] is adopted. This damage surface is expressed as follows:

$$g = \sqrt{\frac{1}{2}Y_{ij}L_{ijkl}Y_{kl}} - (K_0 + K) \tag{53}$$

where K_0 is material constant that demonstrates damage onset. K is thermodynamic conjugate force of φ^{eq} that was expressed through Eq. (34). Y_{ij} is conjugate damage force of φ_{ij} that was expressed through Eq. (30). L_{ijkl} is a fourth order symmetric tensor expressed as follows:

$$L_{ijkl} = \frac{1}{2}\left(\delta_{ik}\delta_{jl} + \delta_{il}\delta_{jk}\right) \tag{54}$$

b) Anisotropic damage growth function

Assuming conjugate damage force of φ_{ij}, that is Y_{ij}, should be always on damage surface ($\dot{g} = 0$); thus, damage consistency is expressed as follows [8, 18]:

$$g \leq 0\,, \quad \dot{\lambda}^d \geq 0\,, \quad \dot{\lambda}^d g = 0 \tag{55}$$

By time derivative of Eq. (53), consistency conditions for damage surface can be expressed as follows:

$$\dot{g} = \frac{\partial g}{\partial Y_{mn}}\dot{Y}_{mn} + \frac{\partial g}{\partial K}\frac{\partial K}{\partial \varphi^{eq}}\dot{\varphi}^{eq} = 0 \tag{56}$$

Differentiating damage surface with respect to Y_{ij} and again with respect to K gives us:

$$\frac{\partial g}{\partial Y_{ij}} = \frac{L_{ijkl}Y_{kl}}{2\sqrt{\frac{1}{2}Y_{mn}L_{mnpq}Y_{pq}}}, \frac{\partial g}{\partial K} = -1 \tag{57), (58}$$

The rate of the equivalent damage ($\dot{\varphi}_{eq}$) is assumed as follows:

$$\dot{\varphi}^{eq} = \sqrt{\dot{\varphi}_{ij}\dot{\varphi}_{ij}} \tag{59}$$

Substituting Eqs. (22) and (57) into Eq. (59) gives us:

$$\dot{\varphi}^{eq} = \sqrt{\frac{L_{mnkl}Y_{kl}L_{mnpq}Y_{pq}}{2Y_{ab}L_{abcd}Y_{cd}}}\left|\dot{\lambda}^d\right| \tag{60}$$

Substituting Eqs. (57), (58) and (60) into Eq. (56), rearranging this equation in terms of $\dot{\lambda}^d$, and considering the fact that the derivative of damage surface with respect to conjugate force of second order damage tensor ($\frac{\partial g}{\partial Y_{mn}}$) and damage loading factor ($\dot{\lambda}^d$) are always positive, gives us [21]:

$$\dot{\lambda}^d = \frac{\frac{\partial g}{\partial Y_{mn}}\dot{Y}_{mn}}{-\frac{\partial g}{\partial K}\frac{\partial K}{\partial \varphi^{eq}}\sqrt{\frac{L_{ijkl}Y_{kl}L_{ijpq}Y_{pq}}{2Y_{ab}L_{abcd}Y_{cd}}}} \tag{61}$$

The time derivative of Y_{ij} gives us:

$$\dot{Y}_{ij} = \frac{\partial Y_{ij}}{\partial \sigma_{kl}}\dot{\sigma}_{kl} + \frac{\partial Y_{ij}}{\partial \varphi_{kl}}\dot{\varphi}_{kl} \tag{62}$$

Substituting Eq. (62) into Eq. (61) and using Eq. (22) gives us:

$$\dot{\varphi}_{rs} = H_{rskl}\dot{\sigma}_{kl} \tag{63}$$

$$H_{rskl} = B^{-1}_{rsij}A_{ijkl} \tag{64}$$

where in these relationships:

$$B_{ijpq} = \delta_{pi}\delta_{qj} - \frac{\frac{\partial g}{\partial Y_{rs}}\frac{\partial Y_{rs}}{\partial \varphi_{pq}}\frac{\partial g}{\partial Y_{ij}}}{\frac{\partial g}{\partial K}\frac{\partial K}{\partial \varphi^{eq}}\sqrt{\frac{L_{mnkl}Y_{kl}L_{mnpq}Y_{pq}}{2Y_{ab}L_{abcd}Y_{cd}}}} \tag{65}$$

And

$$A_{ijkl} = \frac{\frac{\partial g}{\partial Y_{rs}}\frac{\partial Y_{rs}}{\partial \sigma_{kl}}\frac{\partial g}{\partial Y_{ij}}}{\frac{\partial g}{\partial K}\frac{\partial K}{\partial \varphi^{eq}}\sqrt{\frac{L_{mnkl}Y_{kl}L_{mnpq}Y_{pq}}{2Y_{ab}L_{abcd}Y_{cd}}}} \tag{66}$$

These equations demonstrate the relationships between rates of second order damage ($\dot{\varphi}_{ij}$) and rate of stress tensor ($\dot{\sigma}_{ij}$), that are modified in this article. By time derivative of Eq. (7) rate of stress tensor in damaged configuration can be expressed as:

$$\dot{\sigma}_{ij} = E_{ijkl}\dot{\varepsilon}^e_{kl} + \dot{E}_{ijkl}\varepsilon^e_{kl} \tag{67}$$

By considering Eq. (8), E_{ijkl} tensor is a function of φ_{ij}, so:

$$\dot{E}_{ijkl} = \frac{\partial E_{ijkl}}{\partial \varphi_{mn}}\dot{\varphi}_{mn} = 2\, M^{-1}_{ijpq}\bar{E}_{pqrs}\frac{\partial M_{klrs}}{\partial \varphi_{mn}}\dot{\varphi}_{mn} \tag{68}$$

Substituting Eqs. (63) and (68) into Eq. (67) gives us the rate of elastic strain tensor in damaged configuration:

$$\dot{\varepsilon}^e_{ij} = E^{-1}_{ijkl}P_{klmn}\dot{\sigma}_{mn} \tag{69}$$

where:

$$P_{ijkl} = \delta_{ik}\delta_{jl} - \frac{\partial E_{ijmn}}{\partial \varphi_{rs}}H_{rskl}\varepsilon^e_{mn} \tag{70}$$

Fourth order damage tensor (M_{ijkl}) is dependent on second order damage tensor, so the derivative of fourth order damage tensor is expressed as:

$$\dot{M}_{ijkl} = \frac{\partial M_{ijkl}}{\partial \varphi_{mn}}\dot{\varphi}_{mn} \tag{71}$$

The derivative of Eq. (1) gives:

$$\dot{\bar{\sigma}}_{ij} = M_{ijkl}\dot{\sigma}_{kl} + \dot{M}_{ijkl}\sigma_{kl} \tag{72}$$

Afterward, by substituting Eqs. (63) and (71) into Eq. (72) and rearranging, it gives:

$$\dot{\bar{\sigma}}_{ij} = R_{ijkl}\dot{\sigma}_{kl} \tag{73}$$

where:

$$R_{ijkl} = M_{ijkl} + \frac{\partial M_{ijpq}}{\partial \varphi_{rs}}H_{rskl}\sigma_{pq} \tag{74}$$

Equation (73) demonstrates the relationship between rate of stress tensor in damaged and undamaged configurations.

Therefore, the rate of stress tensor in damaged configuration is expressed as:

$$\dot{\sigma}_{ij} = R^{-1}_{ijkl}\dot{\bar{\sigma}}_{kl} \tag{75}$$

c) Yield surface and plastic potential function in damaged configuration

Plastic yield surface and plastic potential function used so far are in undamaged configuration. In this section, plastic yield surface and plastic potential function are mapped to damaged configuration.

By substituting Eq. (1) into Eq. (35), yield surface in damaged configuration is expressed as:

$$f = \frac{c_1}{c_2} - \bar{C} = 0 \tag{76}$$

where:

$$c_1 = \sqrt{\frac{1}{2} Q_{ijkl}\sigma_{kl} Q_{ijmn}\sigma_{mn}} \tag{77}$$

$$c_2 = 1 - \alpha M_{kkij}\sigma_{ij} \tag{78}$$

$$Q_{ijmn} = \left(M_{ijmn} - \frac{M_{kkmn}\delta_{ij}}{3} \right) \tag{79}$$

Derivate plastic yield surface (f) with respect to stress tensor gives us:

$$\frac{\partial f}{\partial \sigma_{ij}} = \frac{Q_{mnij} Q_{mnkl}\sigma_{kl}}{2c_1 c_2} + \frac{\alpha M_{mmij} c_1}{c_2^2} \tag{80}$$

By substituting Eq. (1) into Eq. (37) and deriving with respect to stress tensor, $\partial F^p / \partial \sigma_{ij}$ can be expressed as:

$$\frac{\partial F^p}{\partial \sigma_{ij}} = \frac{Q_{mnij} Q_{mnkl}\sigma_{kl}}{2c_1} \tag{81}$$

Moreover, the rate of plastic strain in damaged configuration is expressed as follows:

$$\dot{\varepsilon}_{ij}^p = \dot{\lambda}^p \frac{\partial F^p}{\partial \sigma_{ij}} \tag{82}$$

Mapping consistency condition in undamaged configuration (Eqs. 50 and 51) to damaged one, gives:

$$\dot{\lambda}^p = \frac{1}{h} \frac{\partial f}{\partial \sigma_{ij}} E_{ijkl} \dot{\varepsilon}_{kl} \tag{83}$$

$$h = \frac{\partial f}{\partial \sigma_{ij}} E_{ijkl} \frac{\partial F^p}{\partial \sigma_{kl}} - \frac{\partial f}{\partial C} \frac{\partial C}{\partial \varepsilon^{ep}} \frac{1 - \alpha I_1 + \alpha\sqrt{3J_2}}{\sqrt{3J_2}} \sigma_{ij} \frac{\partial F^p}{\partial \sigma_{ij}} \tag{84}$$

where, based on experimental examples, $\partial f / \partial \varepsilon^{ep}$ is defined as follows [21]:

$$\frac{\partial f}{\partial \varepsilon^{ep}} = \frac{1}{(1 - \varphi_{eq})} \tag{85}$$

By using Eq. (73) and Eq. (52) the relationship between rate of stress in damaged configuration and rate of strain in undamaged configuration is expressed as follows:

$$\dot{\sigma}_{ij} = C_{ijmn}^{epd} \dot{\bar{\varepsilon}}_{mn} \tag{86}$$

$$C_{ijmn}^{epd} = R_{ijkl}^{-1} \overline{D}_{klmn} \tag{87}$$

All the parameters in Eq. (87) were previously defined.

The damage elastoplastic tangent operator (C_{ijmn}^{epd}) is used in finite element code in order to obtain a new stress or strain increment, using Newton Raphson iterations method.

7. SIMULATION AND VALIDATION

In order to verify the applicability and effectiveness of the proposed model, two nonlinear examples are considered. Results obtained by the proposed model are compared with analogous experimental results and classical plasticity to comprehend its performance. The performance of anisotropic damage model, presented in previous sections, is basically assessed in the simulation of the existing tensile tests of aluminum and graphite cast iron. Numerical tests were conducted by means of displacement control to apply the loads in order to predict hardening and softening in specimens.

In finite element implementation, modified forward Euler integration with error control is used. Forward Euler - explicit - method is appropriate for complex constitutive equations in damage mechanics that need high computational efforts. Forward Euler method is faster than backward Euler – implicit - method. Although conditional stability is the main drawback of explicit method, it can be avoided by selecting suitable time increment steps.

a) Tensile aluminum alloy plate

The tested specimen was a 3.19^{mm} aluminum alloy plate. Fig. 1 shows the geometry of the tensile specimen with 20^{mm} notch radius, tested in a driven machine INSTRON3369 by Brunig et al. [22].

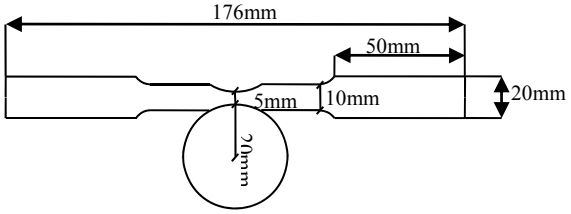

Fig. 1. Tensile aluminum specimen

Material parameters like E, υ and σ_y in both tests are cited from the literature. Using inverse identification procedure, the remaining parameters are obtained. Consequently, using equivalent stress - equivalent plastic strain curves, the first estimates of the material parameters in Eq. (35) are obtained. Subsequently, using inverse identification procedure, finite element simulations of the smooth tension tests have been performed, which lead to the final material parameters.

The material parameters in the simulation are presented in Table 1. These parameters are adapted from Brunig et al. [22].

Table 1. Material parameters considered in the simulation of tensile aluminum alloy plate

Property	Value
Initial Young's modulus, $\bar{E}$ (GPa)	65
Poisson's ratio,υ	0.3
Initial yield strength, σ_y (MPa)	340
Initial isotropic hardening, $\bar{C}_{initial}$ (MPa)	189.7
Material constant in yield surface, α (MPa^{-1})	5e-5
Initial damage surface, K_0 (MPa)	1
Material constant in damage part of Helmholtz free energy function,K_d (MPa)	24
Material constant in plastic part of Helmholtz free energy function, Q (MPa)	350
Material constant in plastic part of Helmholtz free energy function, Bc (MPa)	24

Due to the symmetric condition of specimen, only a quarter of specimen is simulated in numerical model. In order to describe the large stress and deformation gradients anticipated in the necking zone shown in Fig. 2, a spatially non-uniform finite element mesh, composed of 640 higher order (27 nodes) 3D isoperimetric elements has been chosen.

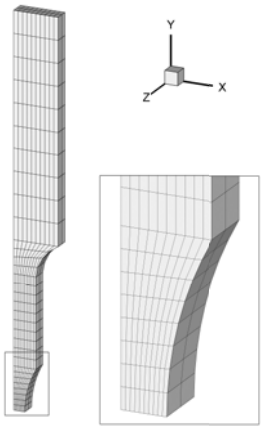

Fig. 2. Finite element mesh of the tensile aluminum specimen

The evolution of the equivalent damage variable field obtained in the finite element analysis is illustrated in the contour plots in Fig. 3a-d. It can be seen that during the early stages of the loading process, maximum damage is detected near the edge of the notch. As the specimen is pulled slowly, the maximum damage zone moves gradually towards the centre of the specimen, and localizes there. At the final stage, damage is highly localized around the centre.

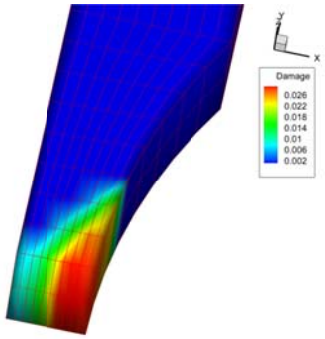

(a) at u/l=1.25%

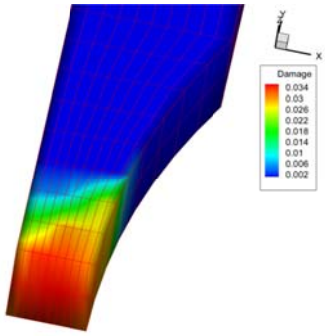

(b) at u/l=1.38%

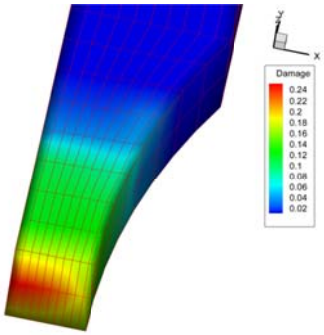

(c) at u/l=2.11%

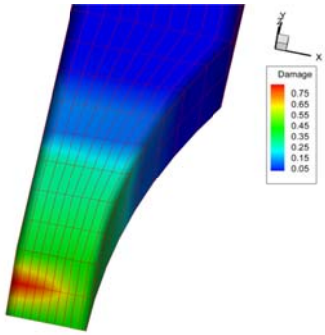

(d) at the end of loading

Fig. 3. Damage contour plots in tensile aluminum specimen

In Fig. 4, contour distribution of stress in the longitudinal of specimen is illustrated at the end of the loading.

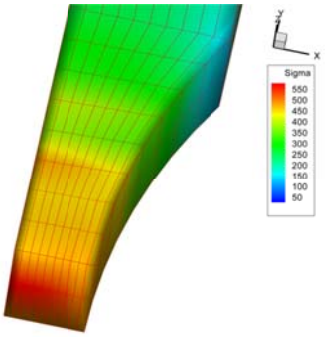

Fig. 4. Longitudinal stress of the tensile aluminum specimen (MPa)

Furthermore, good correlation in load displacement curves between experimental result and numerical simulation can be observed in Fig. 5. In addition, the results obtained from the presented constitutive model are compared with the results from Abaqus software with classical plasticity (Von-Mises) without considering damage, due to the investigative effect of damage on the specimen. In Fig. 5, it is clear that ignoring damage in classical plasticity has a significant effect on the accuracy of the results, and anisotropic damage has the ability to predicate more realistic behavior of the specimen.

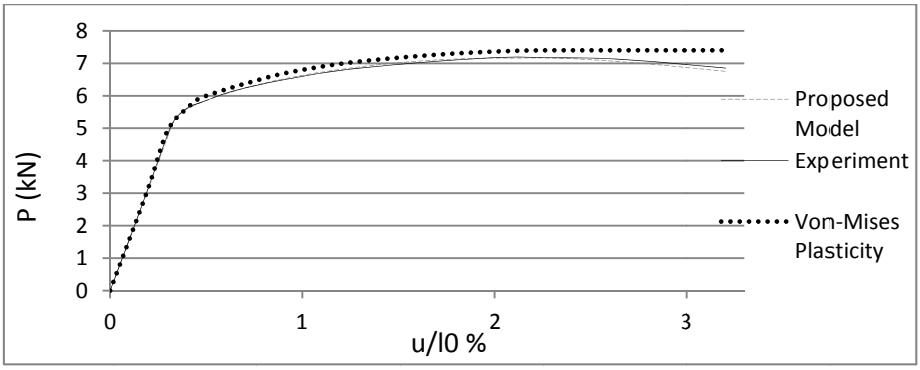

Fig. 5. Axial load (P)-displacement (u) normalized by specimen length curve of the tensile aluminum specimen

Moreover, Fig. 6 shows the thickness change (lateral displacement) versus axial displacement for tensile aluminum alloy plate in critical point. Thickness change is negligible due to small deformation theorem, but damage plasticity model has high ability to demonstrate realistic load displacement curves as shown in Fig. 5.

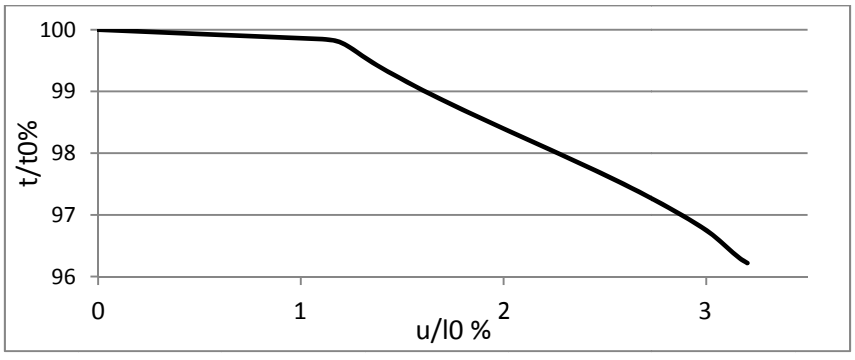

Fig. 6. Thickness change (lateral displacement) versus axial displacement for tensile aluminum specimen

b) Tensile graphite cast iron

Tensile test was performed for the tubular specimen of spheroidized graphite cast iron, and its geometry is shown in Fig. 7. This specimen was tested by Hayakawa et al. [18].

Material parameters are presented in Table 2. These parameters were adapted from Hayakawa et al. [18].

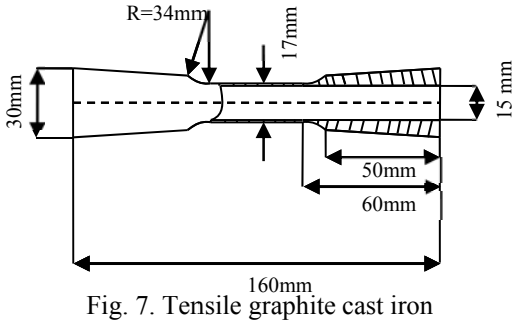

Fig. 7. Tensile graphite cast iron

Table 2. Material parameters considered in the simulation of tensile graphite cast iron

Property	Value
Initial Young's modulus, $\bar{E}$ (GPa)	169
Poisson's ratio, υ	0.285
Initial yield strength, σ_y (MPa)	300
Initial isotropic hardening, $\bar{C}_{initial}$ (MPa)	174.2
Material constant in yield surface, α (MPa^{-1})	1.87e-6
Initial damage surface, K_0 (MPa)	0.22
Material constant in damaged part of Helmholtz free energy function, K_d (MPa)	15.5
Material constant in plastic part of Helmholtz free energy function, Q (MPa)	315
Material constant in plastic part of Helmholtz free energy function, Bc (MPa)	14.2

Due to the symmetric condition of specimen, one eighth of specimen in numerical simulation is used. A spatially non-uniform finite element mesh, composed of 1040 higher order (27 nodes) 3D isoperimetric elements, has been chosen and is shown in Fig. 8.

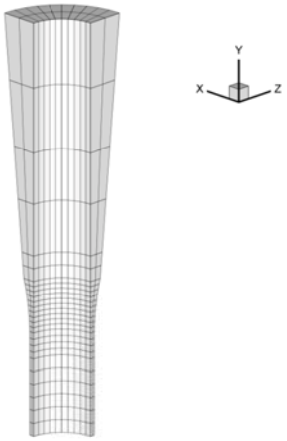

Fig. 8. Finite element mesh of the tensile graphite cast iron

The contour distributions of some characteristics, computed by finite element simulation are presented in Fig. 9a-d. In this test, the onset of damage can be seen in the inner section of the minimum cross section of specimen. The location of the equivalent damage variable field, obtained in each stage of loading, is consistent during the test.

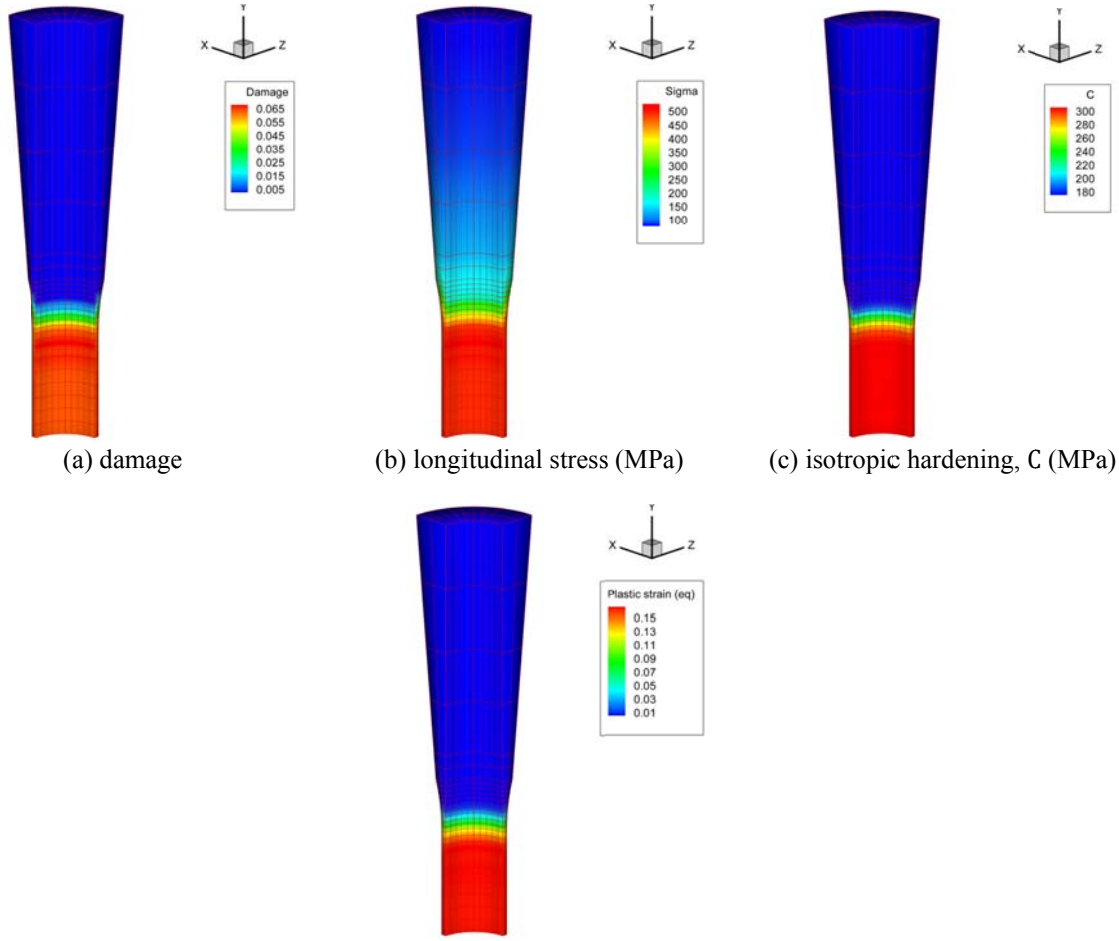

(a) damage (b) longitudinal stress (MPa) (c) isotropic hardening, C (MPa)

(d) effective plastic strain

Fig. 9. Simulation of the tensile graphite cast iron. Computed contour distributions at the end of loading

Figure 10 shows the comparison between the experimental and the predicted results by numerical simulation. In this figure, stress is plotted against strain in critical gauss points that are in the middle of the specimen. It can be seen that the experimental results can be accurately described by the present model. In addition, the results obtained from the presented constitutive model are compared with the results from Abaqus software with classical plasticity (Von-Mises) without considering damage, due to the investigative effect of damage on the specimen. In Fig. 10, it is clear that ignoring damage in classical plasticity has a significant effect on the accuracy of the results, and anisotropic damage has the ability to predicate more realistic behavior of the specimen.

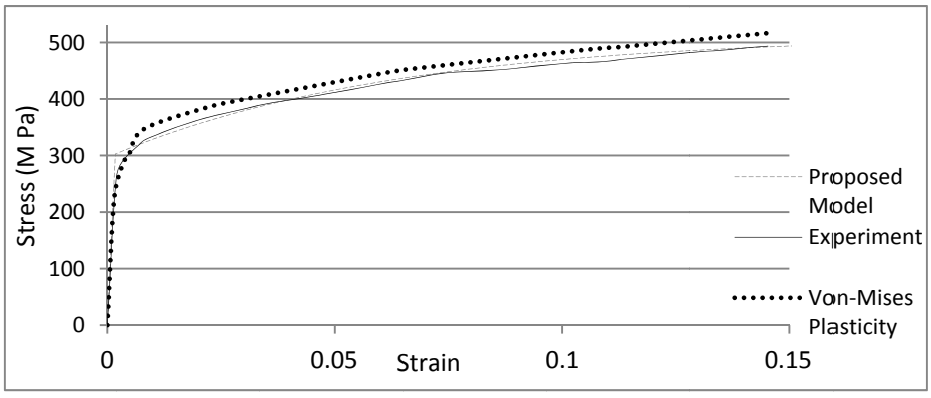

Fig. 10. Experimental and analysis stress strain curves of graphite cast iron under uniaxial tension

Moreover, Fig. 11 shows the thickness change (lateral displacement) versus axial strain for tensile graphite cast iron in critical point.

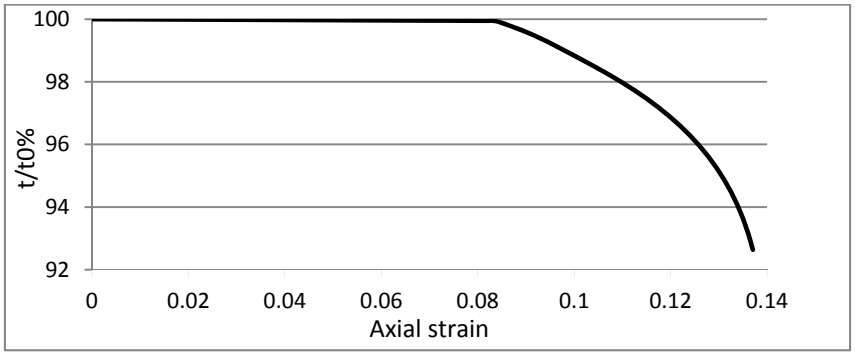

Fig. 11. Thickness change (lateral displacement) versus axial strain for graphite cast iron under uniaxial tension

8. CONCLUSION

In this work, using thermodynamics framework, an anisotropic damage model for iron-based materials is proposed. Damage in metals is described and explained by using: damage tensor for mapping the stresses from the undamaged to the damaged configurations, damage hardening rules (describing damage evolution), and damage conjugate forces (using energy equivalence hypothesis).

Using anisotropic damage, the damage is expressed through a damage mechanics framework to determine the stiffness degradation. In deriving the constitutive model, a yield surface combined with non-associated flow rule is utilized to determine the onset and evolution of plastic strain and a damaged surface with associated flow rule is utilized to determine the onset and evolution of damage. Therefore, this model has the ability to demonstrate growth of anisotropic damage besides plastic deformations in iron based materials.

Numerical simulations of some existing experiments, including tensile tests on specimens of aluminum alloy plate and graphite cast iron have been performed, and the corresponding numerical results are validated with the experimental measurements.

REFERENCES

1. Murakami, S. (1985). Damage mechanics and its recent development. *JSME*, Vol. A51, pp. 1651-1659.
2. Lemaitre, J. (1992). *A short course in damage mechanics*. Springer-Verlag, New York.
3. Kachanov, L. M. (1958). On rupture time under condition of creep. *Izvestia Akademi Nauk USSR, Otd,Techn. Nauk, Moskwa*, Vol. 8, pp. 26–31.
4. Habibi, A. R., Izadpanah, M. & Yazdani, A. (2013). Inelastic damage analysis of RCMRFS using pushover method. *Iranian Journal of Science & Technology, Transactions of Civil Engineering*, Vol. 37, No. C2, pp. 345–352.
5. Chow, C. L. & Wang, J. (1988). A finite element analysis of continuum damage mechanics for ductile fracture. *Int. J. Fracture*, Vol. 38, pp. 83–102.
6. Krajcinovic, D. (1983a). Continuum damage mechanics. *J. Appl. Mech.-T ASME*, Vol. 37, pp. 1–6.
7. Salehi, M., Ziaei rad, S., Ghayour, M. & Vaziry, M. A. (2011). A non model-based damage detection technique using dynamically measured flexibility matrix. *Iranian Journal of Science & Technology, Transaction B*: *Engineering*, Vol. 35, pp. 1–13.

8. Ju, J. W. (1990). Isotropic and anisotropic damage variables in continuum damage mechanics. *J. Eng. Mech.-ASCE*, Vol. 116, pp. 2764–2770.
9. Menzel, A., Ekh, M., Runesson, K. & Steinmann, P. (2005). A framework for multiplicative elastoplasticity with kinematic hardening coupled to anisotropic damage. *Int. J. Plasticity*, Vol. 21, pp. 397–434.
10. Cordebois, J. P. & Sidoroff, F. (1979). Anisotropic damage in elasticity and plasticity, *J. Theor. App. Mech-Pol, Numero special*, pp. 40–45.
11. Voyiadjis, G. Z. & Kattan, P. I. (2006). *Advances in damage mechanics: metals and metal matrix composites, with an introduction to fabric tensors*. second ed., Elsevier, Oxford.
12. Voyiadjis, G. Z. & Dorgan, R. J. (2007). Framework using functional forms of hardening internal state variables in modeling elasto-plastic-damage behavior. *Int. J. Plasticity*, Vol. 23, pp. 1826–1859.
13. Chow, C. L. & Wang, J. (1987). An anisotropic theory of elasticity for continuum damage mechanics. *INT. J. FRACTURE*, Vol. 33, pp. 2–16.
14. Malvern, E. (1989). *Introduction to the mechanics of a continuous medium*. Prentice Hall.
15. Chaboche, J. L. (1989). Constitutive equations for cyclic plasticity and cyclic viscoplasticity. *Int. J. Plasticity*, Vol. 5, pp. 247–302.
16. Rice, J. R. (1971). Inelastic constitutive relation for solids: an internal variable theory and its application to metal plasticity. *J. Mech. Phys. Solids*, Vol. 19, pp. 433-455.
17. Chen, W. F. & Zhang, H. (1988). *Structural plasticity*. Springer-Verlag, New York.
18. Hayakawa, K., Murakami, S. & Liu, Y. (1998). An irreversible thermodynamics theory for elastic–plastic-damage materials. *Eur. J. Mech. A-Solid*, Vol. 17, pp. 13–32.
19. Spitzig, W. A., Sober, R. J. & Richmond, O. (1975). Pressure dependence of yielding and associated volume expansion in tempered martensite. *Acta Metall Mater.*, Vol. 23, pp. 885–893.
20. Spitzig, W. A. & Richmond, O. (1984). The effect of pressure on the flow stress of metals. *Acta Metall Mater.*, Vol. 32, pp. 457–463.
21. Voyiadjis, G. Z., Taqieddin, Z. N. & Kattan, P. I. (2008). Anisotropic damage–plasticity model for concrete. *Int. J. Plasticity*, Vol. 24, pp. 1946–1965.
22. Brunig, M., Chyra, O., Albrecht, D., Driemeier, L. & Alves, M. (2008). A ductile damage criterion at various stress triaxialities. *Int. J. Plasticity*, Vol. 24, pp. 1731–1755.